AUTOPHAGY
2020, VOL. 16, NO. 6, 1130–1142
https://doi.org/10.1080/15548627.2019.1660545

Taylor & Francis
Taylor & Francis Group

RESEARCH PAPER

Modulating EGFR-MTORC1-autophagy as a potential therapy for persistent fetal vasculature (PFV) disease

Meysam Yazdankhah[a], Peng Shang[a], Sayan Ghosh[a], Imran A. Bhutto[a], Nadezda Stepicheva[a], Rhonda Grebe [b], Stacey Hose[a], Joseph Weiss[a], Tianqi Luo[b], Subrata Mishra[b], S. Amer Riazuddin[b], Arkasubhra Ghosh[c], James T. Handa[b], Gerard A. Lutty[b], J. Samuel Zigler Jr[b], and Debasish Sinha[a,b]

[a]Glia Research Laboratory, Department of Ophthalmology, University of Pittsburgh School of Medicine, Pittsburgh, PA, USA; [b]The Wilmer Eye Institute, The Johns Hopkins University School of Medicine, Baltimore, MD, USA; [c]GROW Research Laboratory, Narayana Nethralaya Foundation, Bengaluru, India

ABSTRACT

Persistent fetal vasculature (PFV) is a human disease that results from failure of the fetal vasculature to regress normally. The regulatory mechanisms responsible for fetal vascular regression remain obscure, as does the underlying cause of regression failure. However, there are a few animal models that mimic the clinical manifestations of human PFV, which can be used to study different aspects of the disease. One such model is the Nuc1 rat model that arose from a spontaneous mutation in the *Cryba1* (crystallin, beta 1) gene and exhibits complete failure of the hyaloid vasculature to regress. Our studies with the Nuc1 rat indicate that macroautophagy/autophagy, a process in eukaryotic cells for degrading dysfunctional components to ensure cellular homeostasis, is severely impaired in Nuc1 ocular astrocytes. Further, we show that CRYBA1 interacts with EGFR (epidermal growth factor receptor) and that loss of this interaction in Nuc1 astrocytes increases EGFR levels. Moreover, our data also show a reduction in EGFR degradation in Nuc1 astrocytes compared to control cells that leads to over-activation of the mechanistic target of rapamycin kinase complex 1 (MTORC1) pathway. The impaired EGFR-MTORC1-autophagy signaling in Nuc1 astrocytes triggers abnormal proliferation and migration. The abnormally migrating astrocytes ensheath the hyaloid artery, contributing to the pathogenesis of PFV in Nuc1, by adversely affecting the vascular remodeling processes essential to regression of the fetal vasculature. Herein, we demonstrate *in vivo* that gefitinib (EGFR inhibitor) can rescue the PFV phenotype in Nuc1 and may serve as a novel therapy for PFV disease by modulating the EGFR-MTORC1-autophagy pathway.

Abbreviations: ACTB: actin, beta; CCND3: cyclin 3; CDK6: cyclin-dependent kinase 6; CHQ: chloroquine; COL4A1: collagen, type IV, alpha 1; CRYBA1: crystallin, beta A1; DAPI: 4′6-diamino-2-phenylindole; EGFR: epidermal growth factor receptor; GAPDH: glyceraldehyde-3-phosphate dehydrogenase; GFAP: glial fibrillary growth factor; KDR: kinase insert domain protein receptor; MAP1LC3/LC3: microtubule-associated protein 1 light chain 3; MKI67: antigen identified by monoclonal antibody Ki 67; MTORC1: mechanistic target of rapamycin kinase complex 1; PARP: poly (ADP-ribose) polymerase family; PCNA: proliferating cell nuclear antigen; PFV: persistent fetal vasculature; PHPV: persistent hyperplastic primary vitreous; RPE: retinal pigmented epithelium; RPS6: ribosomal protein S6; RPS6KB1: ribosomal protein S6 kinase, polypeptide 1; SQSTM1/p62: sequestome 1; TUBB: tubulin, beta; VCL: vinculin; VEGFA: vascular endothelial growth factor A; WT: wild type.

ARTICLE HISTORY
Received 30 November 2018
Revised 26 July 2019
Accepted 3 August 2019

KEYWORDS
Astrocytes; autophagy; CRYBA1 (ßA3/A1-crystallin); EGFR (epidermal growth factor receptor); gefitinib; hyaloid vessels; lysosomes; MTORC1 (mechanistic target of rapamycin complex 1); Nuc1 rat; persistent fetal vasculature (PFV) disease

Introduction

The eye has a unique transient vascular system, the hyaloid (or fetal) vasculature, which nourishes the lens and retina during ocular development [1–3]. After the formation of retinal vessels, the fetal vasculature normally regresses to remove light scattering elements from the visual path [4,5]. Persistent fetal vasculature (PFV), previously known as persistent hyperplastic primary vitreous (PHPV), a human disease in which this vascular structure fails to regress normally, can lead to serious congenital pathologies [6,7]. The exact prevalence of PFV is unknown; however, a study on childhood blindness and visual loss found that PFV accounts for about 5% of childhood blindness [8,9]. We previously reported that in the Nuc1 rat, a spontaneous mutant with a variety of developmental ocular abnormalities, there was persistence of the entire fetal vasculature [10,11]. A 27 base pair insertion in exon 6 of *Cryba1*, the gene mutated in Nuc1, encodes CRYBA1, which is a highly abundant structural protein in the lens [12,13]. While several mutations in *Cryba1* cause cataract in humans, PFV has not been reported in any of these patients [14,15]. In fact, no mutation in an eye specific gene has been associated with PFV disease.

Cryba1 is also expressed in astrocytes, cells that are critical to vascular development in the retina, but have not been thought to be involved in either the formation or regression of the hyaloid vasculature [12,16–18]. We showed in the Nuc1 rat, and in

CONTACT Debasish Sinha debasish@jhmi.edu;debasish@pitt.edu Departments of Ophthalmology, Cell Biology and Developmental Biology, Children's Hospital of University of Pittsburgh School of Medicine, One Children's Hospital Drive, 4401 Penn Avenue, Pittsburgh, PA 15224, USA
Supplemental data for this article can be accessed here.

human samples from PFV patients, that astrocytes abnormally ensheath the hyaloid artery [19]. Several other mouse models that exhibit PFV also appear to have astrocytes associated with the persistent hyaloid artery [20–22]. Further, in transgenic mice overexpressing the mutant (Nuc1) CRYBA1 specifically in astrocytes, these astrocytes also migrate into the vitreous and ensheath the hyaloid artery [23]. Therefore, we postulated that these glial cells are causally involved in persistence of the hyaloid artery.

It is well established that EGFR (epidermal growth factor receptor) plays a critical role in normal cell growth and development [24]. However, overexpression of this receptor, which regulates cell proliferation and migration, is also a hallmark of a variety of tumor cells [25–27]. Importantly, a major downstream effector of EGFR is the mechanistic target of rapamycin kinase complex 1 (MTORC1), the principal regulator of macroautophagy/autophagy [26,27]. In this study, we demonstrate that gefitinib may serve as a novel therapy for PFV by modulating the EGFR-MTORC1-autophagy pathway, which can regulate vascular regression and abnormal astrocyte proliferation and migration.

Results

Loss of CRYBA1 in Nuc1 accelerated the rate of astrocyte proliferation and migration

We show that cultured Nuc1 astrocytes migrate and proliferate faster than wild type astrocytes (Figure 1A–C, Figure S1A–B). In addition, the expression pattern of the cell proliferation marker MKI67 and the levels of cell cycle regulators CCND3 and CDK6 are significantly increased in Nuc1 astrocytes compared to wild type (Figure S1C–G). This abnormal proliferation and migration can be rescued by overexpressing *Cryba1* in the Nuc1 cells (Figure 1A,B,D), providing evidence that CRYBA1 regulates proliferation and migration in ocular astrocytes. Our data consistently show proliferating astrocytes in Nuc1 retina, while wild type astrocytes were rarely found to be proliferating in the postnatal 31-d-old retina. Moreover, the level of MKI67 in astrocytes and the expression of PCNA (cell proliferation marker) were much higher in Nuc1 retina relative to wild type (Figure S2A–C).

Nuc1 astrocytes showed activation of MTORC1 and decreased autophagy that can be rescued upon treatment with AZD8055 (MTOR inhibitor)

Our data show upregulation of MTORC1 in Nuc1 astrocytes compared to astrocytes from wild type controls (Figure 2A–D). Overexpressing *Cryba1* can reduce this overactivation of MTORC1 (indicated by decline in p-RPS6KB1) in Nuc1 astrocytes. A similar effect was not observed in wild type cells (Figure 2E,F). Moreover, exposure of cultured astrocytes (wild type and Nuc1) to chloroquine, which blocks autophagosome degradation, increased the level of LC3-II, a marker generally used to assess autophagy [28,29] (Figure 2G,H). As seen in the histogram, the LC3-II flux in the Nuc1 cells was just 66% of the normal rate. We also observed that the levels of SQSTM1 [30], a receptor for cargo

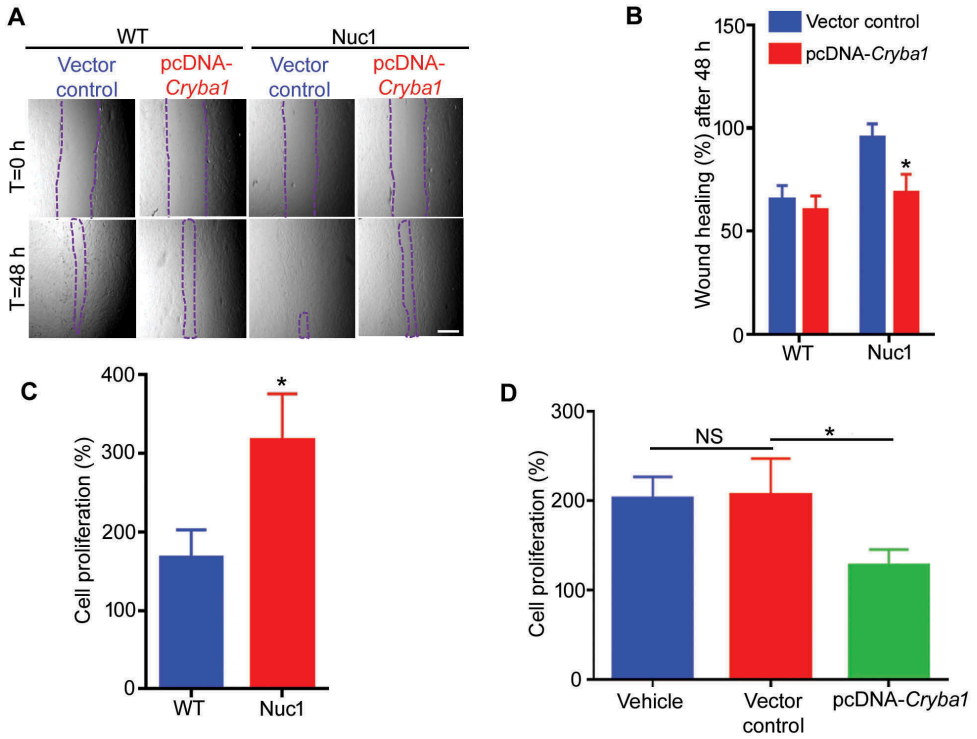

Figure 1. Increased proliferation and migration of Nuc1 astrocytes. (A,B). The rate of migration of Nuc1 astrocytes was significantly higher than WT cells as indicated by the wound healing assay (area denuded of cells is demarcated by dashed lines). Migration was significantly reduced in the Nuc1 cells when *Cryba1* (pcDNA-*Cryba1*) was overexpressed. Empty vector had no effect. There was no significant difference in wound closure for WT cells after over-expression of *Cryba1*. Scale bar: 70 µm. (C) Proliferation rates of WT and Nuc1 astrocytes were measured by counting the total number of cells after 72 h in culture and dividing by the initial number of cells. Nuc1 astrocytes proliferated approximately twice as fast as WT. (D) Overexpression of *Cryba1* in the Nuc1 cells led to a reduction of proliferation. Empty vector had no effect. All experiments were repeated 3 times. Values are mean ± SEM. * $P < 0.05$; NS = not significant.

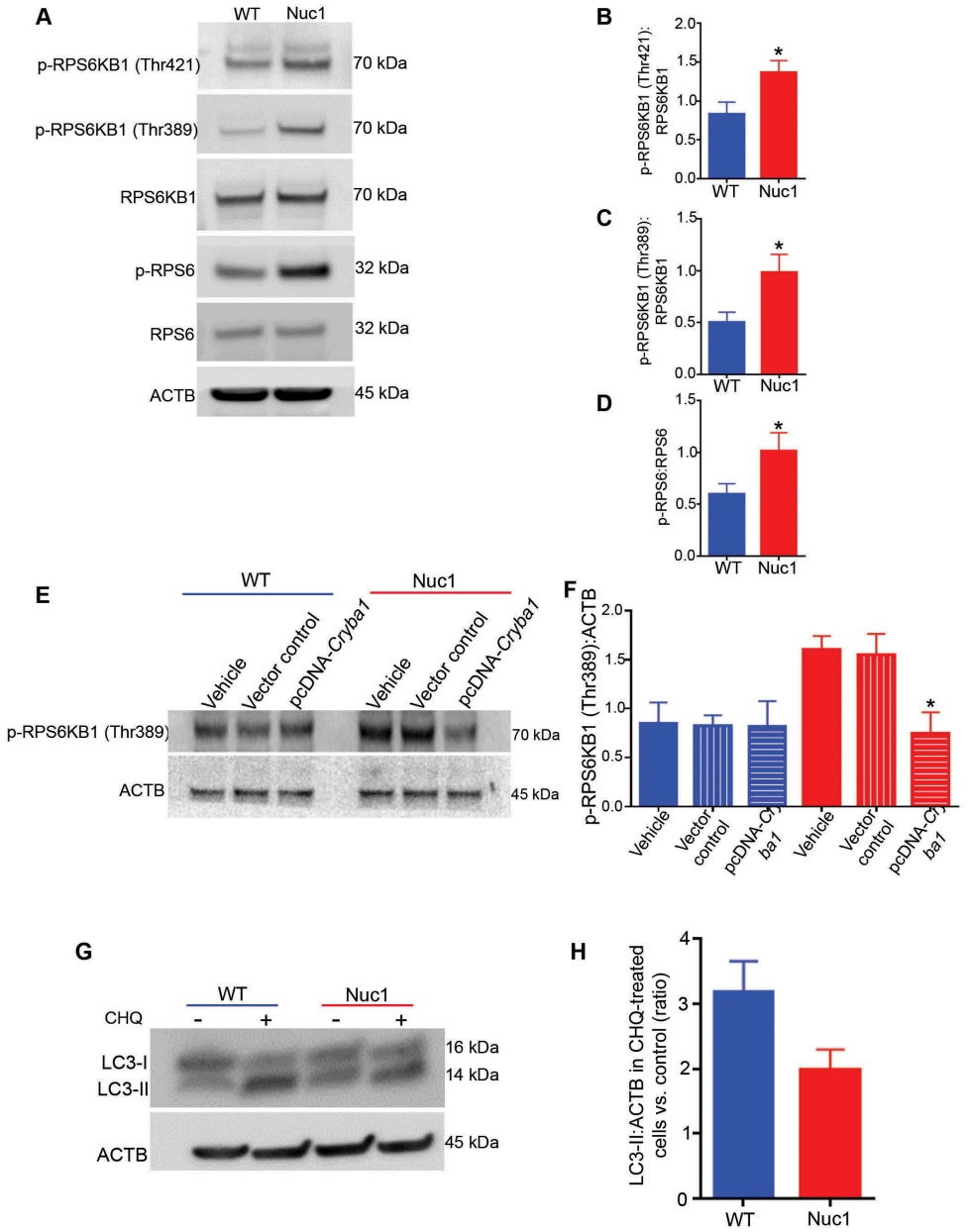

Figure 2. Over-activation of the MTORC1 pathway and downregulation of autophagy in Nuc1 astrocytes. (A–D) Astrocytes were isolated and cultured from Nuc1 and WT optic nerves. Protein lysates were prepared and analyzed by immunoblotting for activation markers of the MTORC1 pathway. Although the levels of total RPS6KB1 and RPS6 were not different between the two groups, Nuc1 astrocytes showed a significant increase in two different phosphorylated (active) forms of RPS6KB1 and phosphorylated-RPS6 compared with WT. The graphs represent the ratio of phosphorylated proteins:total proteins in WT and Nuc1 astrocytes. (E,F) The level of phospho-RPS6KB1 was significantly reduced in the Nuc1 astrocytes when *Cryba1* (pcDNA-*Cryba1*) was overexpressed. However, a similar effect was not seen in WT cells. Empty vector had no effect. (G,H) Astrocytes from WT and Nuc1 optic nerves were cultured in the presence or absence of the lysosomal inhibitor chloroquine (CHQ). The cells were then lysed and protein lysates analyzed for LC3 by immunoblotting. A significant decrease in the accumulation of the autophagosome-positive LC3-II isoform was observed in Nuc1 cells relative to WT after CHQ treatment. The graphs represent mean ± SEM from 3 independent experiments repeated in triplicate. * $P < 0.05$; NS, not significant.

destined to be degraded by autophagy, were higher in Nuc1 astrocytes than in controls (Figure S3A,B,E,F), consistent with the accumulation of undegraded cargo. Importantly, overexpressing CRYBA1 in Nuc1 astrocytes rescued SQSTM1 expression levels (Figure S3C,D,G,H). Moreover, our data showed that SQSTM1 was highly expressed in the astrocytes of Nuc1 retina relative to wild type. (Figure S4 A–C).

We then used the tandem sensor RFP-GFP-LC3 to compare the number of autophagosomes and autolysosomes in wild type and Nuc1 astrocytes (Figure 3A,B). By combining an acid-sensitive GFP with an acid-insensitive RFP, the conversion from autophagosome (neutral pH) to autolysosome (acidic pH) was visualized by imaging the specific loss of the GFP fluorescence. Live cell imaging showed mostly red puncta (autolysosomes) in wild type cells, with some yellow puncta (autophagosomes) present. When wild type cells were treated with bafilomycin A_1 (an inhibitor of V-ATPase) to inhibit lysosomal acidification, the number of yellow puncta increased, indicating the failure of the normal processing of autophagosomes. When Nuc1 cells were imaged, we found

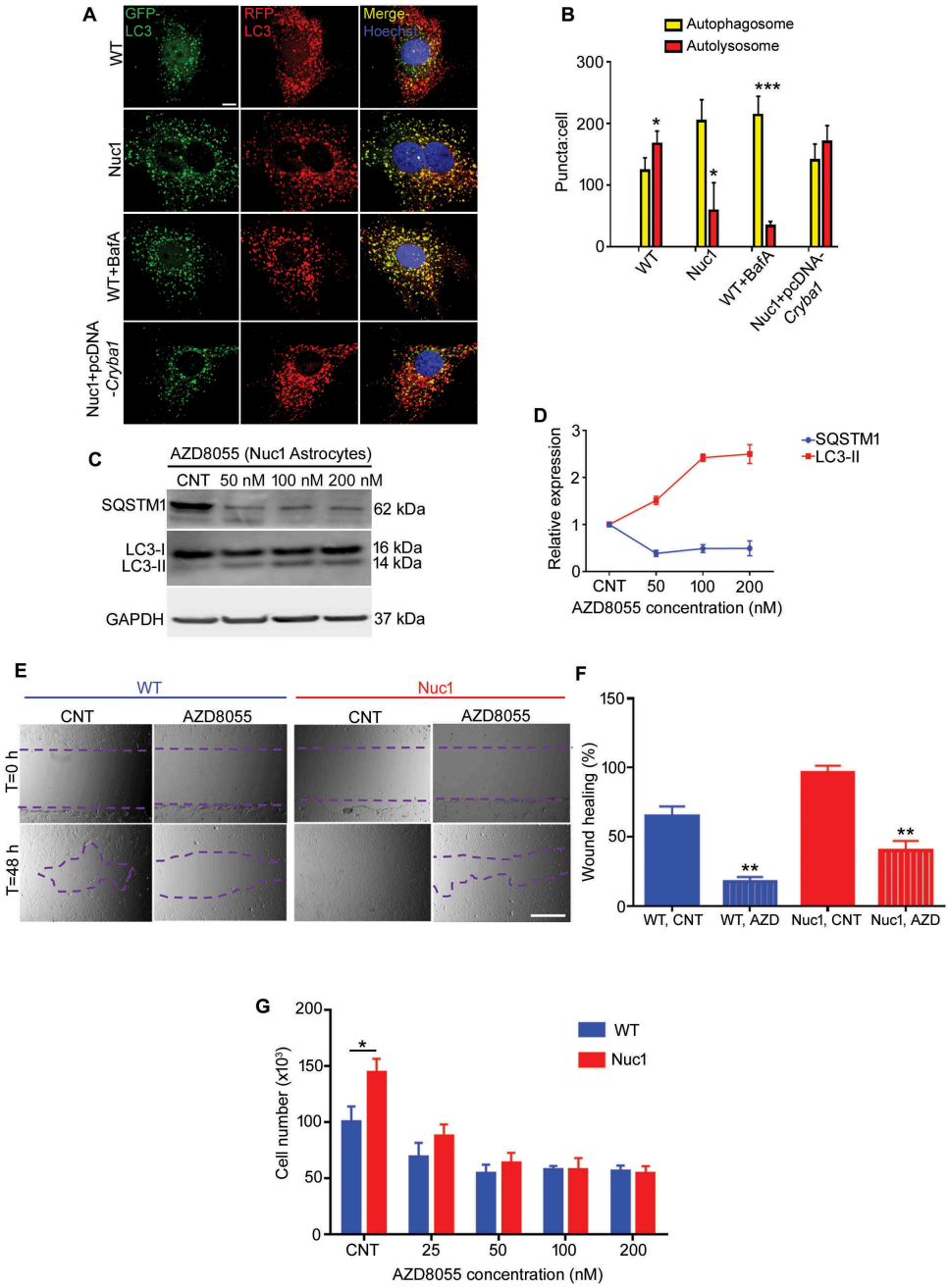

Figure 3. Impairment of autophagosome clearance in Nuc1 astrocytes. (A,B) Astrocytes were transduced by RFP–GFP tandem fluorescent-tagged LC3 (RFP–GFP–LC3) construct and then serum starved. Yellow puncta correspond to autophagosomal structures since both GFP and RFP fluoresce at cytoplasmic pH. Red puncta represent autolysosomes because GFP is quenched by the acidity of lysosomes. Merged confocal images demonstrated that most puncta were red in WT cells indicating that GFP had been quenched in lysosomes: in contrast, most puncta were yellow in Nuc1 astrocytes. A similar pattern was observed in WT cells when the lysosomal function was blocked by BafA1. Further, overexpressing *Cryba1* (pcDNA-*Cryba1*) in Nuc1 cells led to an increase in number of autolysosomes to near WT levels. The numbers of autophagosomes and autolysosomes were quantified from 30 images per group for each experiment. Scale bar: 20 µm. (C,D) Western blotting analysis of the autophagy markers (SQSTM1 and LC3) in cellular extracts from Nuc1 astrocytes grown in normal media (CNT) or in media containing different concentrations of AZD8055 (MTOR inhibitor) for 12 h. GAPDH was used as loading control. AZD8055 induced autophagy in Nuc1 astrocytes, since levels of SQSTM1 decreased and LC3-II increased in a dose-dependent manner. (E,F) Wound healing assay was performed on Nuc1 and WT astrocytes grown in normal medium (CNT) or in medium containing AZD8055 (50 nM). Phase-contrast photomicrographs (10× objective) were acquired at T = 0 and 48 h after scratching. The level of cellular migration in both WT and Nuc1 astrocytes was highly reduced by AZD8055. Scale bar: 70 µm. (G) AZD8055 impeded cell proliferation of Nuc1 and WT astrocytes. All cultures were started with an identical number of cells (6.5×10^4 cells/ml) and the total number of cells was counted after 72 h. Graphs represent mean ± SEM from a triplicate experiment, representative of at least 3 independent experiments. * $P < 0.05$; ** $P < 0.01$; *** $P < 0.001$.

predominantly yellow puncta. Indeed, we have previously reported that the pH in Nuc1 lysosomes is higher than wild type [18,31]. Importantly, when *Cryba1* was overexpressed in Nuc1 astrocytes, yellow puncta decreased and red puncta predominated, indicating recovery of normal processing of autophagosomes. Interestingly, inhibition of the MTORC1 pathway by the potent inhibitor AZD8055 [32,33] results in activation of the autophagy pathway in Nuc1 astrocytes, as indicated by increased autophagy flux (increased LC3-II turnover), and decreased levels of SQSTM1 (Figure 3C,D).

AZD8055 treatment of wild type astrocytes also led to significant reduction of SQSTM1 levels (Figure S5A,B). In addition, we showed that while AZD8055 can rescue the abnormally high proliferation and migration rates of Nuc1 astrocytes, it also decreases the rates of these processes in wild type astrocytes (Figure 3E–G).

CRYBA1 interacted with EGFR and reduction of EGFR degradation led to activation of the MTORC1 pathway in Nuc1 astrocytes

In a recent human proteome high-throughput protein array, we identified EGFR as a possible interacting partner of CRYBA1 [34]. Here, we show that in a pulldown assay, CRYBA1 binds to EGFR in primary rat astrocytes (Figure 4A,B). Western analysis indicated that the level of EGFR is higher in Nuc1 astrocytes compared to wild type controls (Figure 4C,D). Also, overexpression of *Cryba1* in Nuc1 astrocytes rescued EGFR to normal levels, indicating that CRYBA1 regulates the levels of EGFR in astrocytes (Figure 4E,F). Moreover, studies on retinas from Nuc1 rats showed a significant increase in expression of EGFR, relative to wild type. (Figure S6A,B).

Immuno-electron microscopy studies using an antibody to EGFR showed accumulation of EGFR in the lysosomes of Nuc1 astrocytes, but not in wild type cells (Figure 5A). *In vitro* studies by blocking lysosomal function with chloroquine clearly showed that in Nuc1 astrocytes, lysosomal-mediated degradation of EGFR is reduced relative to normal astrocytes (Figure 5B,C). Further, exposing wild type astrocytes to chloroquine increased the levels of p-EGFR, p-RPS6KB1 and p-RPS6 even after stimulation with EGF, since lysosomal-mediated clearance was compromised (Figure 5D). As expected, we also observed that the turnover rate of RPS6 was significantly higher in wild type astrocytes exposed to chloroquine than in Nuc1, further confirming that Nuc1 astrocytes have an inherent defect in lysosomal-mediated clearance (Figure 5E,F). Moreover, stimulating wild type and Nuc1 cells with EGF indicated rapid clearance of EGFR in wild type astrocytes, but not in Nuc1 astrocytes (Figure 5G,H).

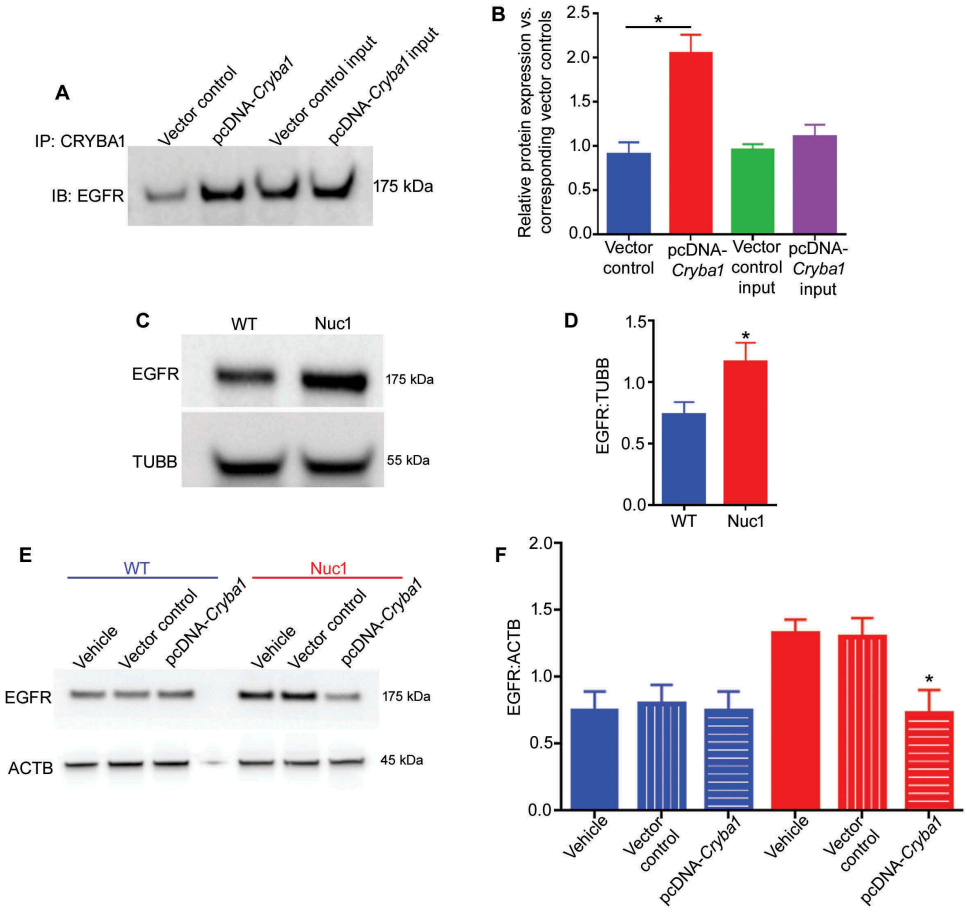

Figure 4. An increased level of EGFR in Nuc1 astrocytes. (A,B) To detect EGFR and CRYBA1 association, *Cryba1* was overexpressed in WT astrocytes by transfecting with pcDNA-*Cryba1* for 48 h. Non-targeted pcDNA was used as vector control. Co-immunoprecipitation followed by immunoblotting on lysates from cultured astrocytes showed increased association of CRYBA1 with EGFR in cells transfected with the overexpression vector relative to vector control group. No significant change was observed among the input controls. (C,D) An increased level of EGFR was clearly visible in Nuc1 cells relative to WT. TUBB was used as loading control. (E, F) The level of EGFR was diminished in Nuc1 cells, but not in WT astrocytes, when *Cryba1* (pcDNA-*Cryba1*) was overexpressed. Empty vector had no effect. ACTB was used as loading control. Values are plotted as mean ± SEM from 3 independent experiments repeated in triplicate. * $P < 0.05$; NS = not significant.

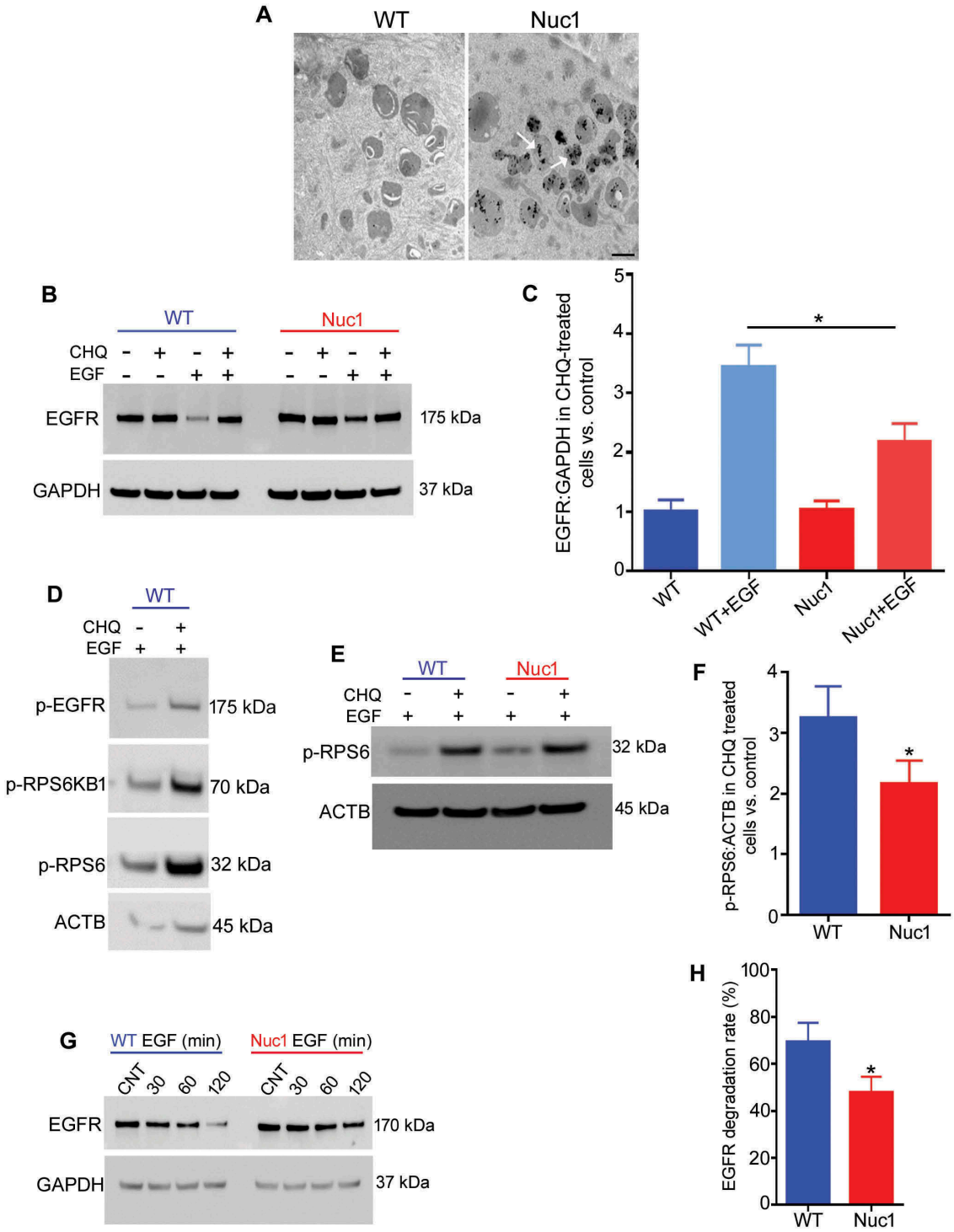

Figure 5. Impairment of lysosomal activity in Nuc1 astrocytes leads to reduction of EGFR degradation and sustained MTOR pathway activation. (A) Immuno-electron microscopy revealed marked accumulation of EGFR in lysosomes of Nuc1 cells relative to WT (white arrows). Scale bar: 800 nm. (B,C) EGF-induced EGFR degradation in WT and Nuc1 astrocytes after 2 h in the presence or absence of the lysosomal inhibitor, CHQ. Proteins were extracted and analyzed by immunoblot for EGFR. The level of EGFR decreased after EGF (100 ng/mL) treatment whereas this decrease was eliminated by the lysosomal inhibitor CHQ. Less accumulation of EGFR was observed in Nuc1 cells after CHQ treatment (50 μM) compared to WT. GAPDH was used as loading control. (D) WT astrocytes were treated with EGF or combination of EGF and CHQ for one h, and then cell lysates were subjected to immunoblotting. After CHQ treatment, phospho-EGFR was increased, consistent with similar increases in phospho-RPS6KB1 and phospho-RPS6. (E,F) Under the same conditions, the level of EGF-stimulated phospho-RPS6 was higher in Nuc1 cells indicating impairments in lysosome-mediated clearance. Thus, the level of phospho-RPS6 turnover (EGF+CHQ:EGF) in Nuc1 cells was decreased compared to WT. ACTB was used as a control. (G,H) WT and Nuc1 astrocytes were stimulated by exogenous EGF (100 ng/mL), lysed, and EGFR level determined by western blot. GAPDH was used as a control. The rate of EGFR degradation after 120 min EGF stimulation was calculated as follows [CNT- after 120 min/CNT] × 100. The degradation rate of EGFR was significantly lower in Nuc1 cells relative to WT. In all panels, graphs show mean ± SEM from 3 individual experiments repeated in triplicate. * $P < 0.05$.

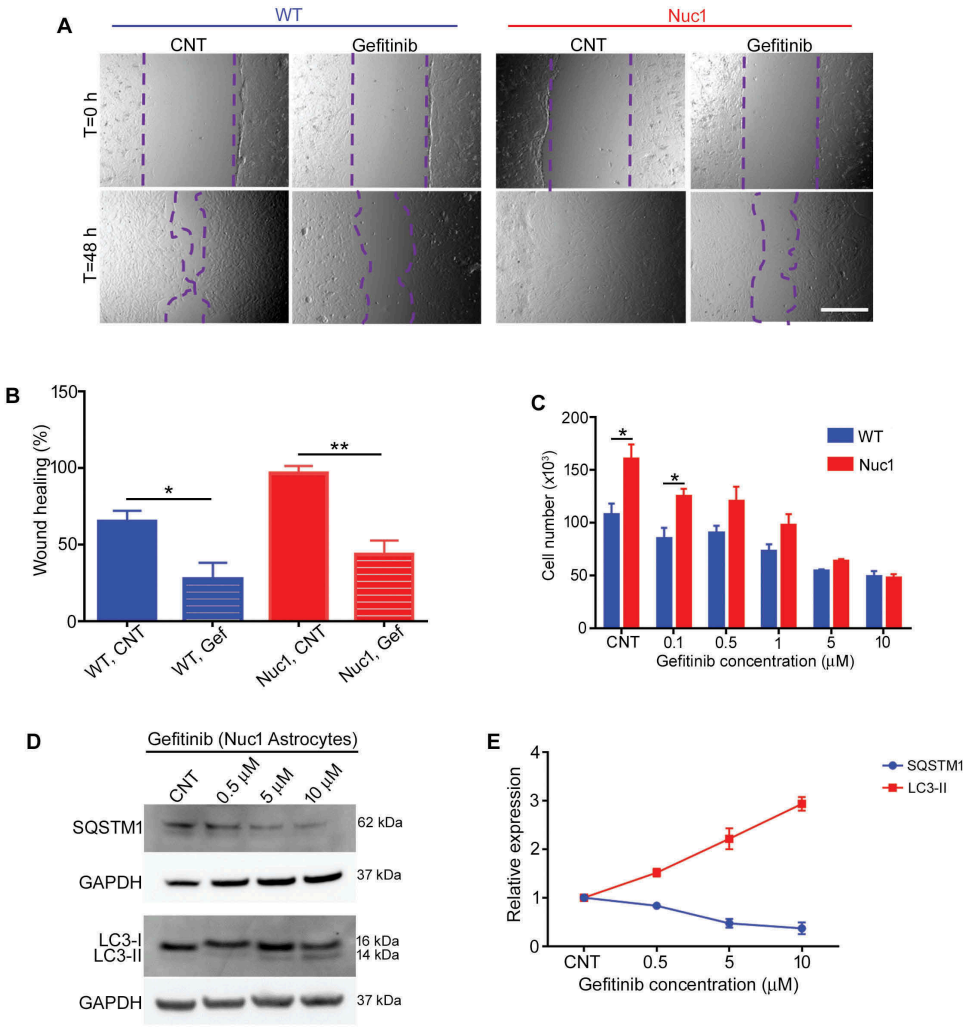

Figure 6. Effect of gefitinib on proliferation and migration of Nuc1 astrocytes in culture. (A,B) Wound healing assay was performed on Nuc1 and WT astrocytes grown in normal medium (CNT) or in medium containing gefitinib (5 μM). Phase-contrast photomicrographs (10× objective) were acquired at T = 0 and 48 h after scratching. The level of cellular migration in both WT and Nuc1 astrocytes was reduced by approximately 60% after gefitinib treatment. Scale bar: 70 μm. (C) Gefitinib inhibited proliferation of Nuc1 and WT astrocytes. All cultures were started with an identical number of cells (6.5×10^4 cells/ml) and the total number of cells was counted after 72 h. (D,E) Western blotting analysis was used to quantify the expression of autophagy markers (SQSTM1 and LC3-II) in cellular extracts from Nuc1 astrocytes grown in normal media (CNT) or with different concentrations of gefitinib for 12 h. GAPDH was used as loading control. Gefitinib induced autophagy in Nuc1 astrocytes, since levels of SQSTM1 decreased and LC3-II increased as a function of dose. Values are mean ± SEM from 3 independent experiments. * $P < 0.05$; ** $P < 0.01$.

Gefitinib (EGFR inhibitor) and rapamycin (MTORC1 inhibitor) rescued abnormally increased proliferation and migration in Nuc1 astrocytes and also reduced severity of the PFV phenotype in Nuc1

When Nuc1 astrocytes were treated with gefitinib [35], both migration and proliferation rates were rescued (Figure 6A–C). However, the decrease in cell number following drug treatment is caused by cessation of proliferation (Figure S7A,B,F,G), not induction of cell death (Figure S7C,D,E,G,H). Further, we observed a dose-dependent decrease in SQSTM1 and an increase in autophagy flux (Figure 6D,E). Gefitinib treatment increased the level of autophagy in Nuc1 astrocytes to near wild type cell levels (Figure S8A,B). In fact, when gefitinib or rapamycin was injected intraperitoneally into Nuc1 rats to test our notion that such treatment would block the EGFR-MTORC1-autophagy pathway and rescue the PFV phenotype in Nuc1, we found that either gefitinib (Figure 7A–C) or rapamycin (Figure S9A,B) treatment significantly reduced retention of the hyaloid artery. Moreover, gefitinib or rapamycin treatment led to a reduction in proliferation (PCNA) and an increase in autophagy (indicated by a reduction in SQSTM1 levels) in Nuc1 retina (Figure S10A–C). Additionally, the reduced levels of EGFR seen after gefitinib or rapamycin treatment (Figure S11A,B) were likely a consequence of inhibited proliferation and a decreased number of astrocytes. For PFV patients, targeting the EGFR-MTORC1-autophagy pathway with gefitinib (Figure 8) may be an effective means of blocking the abnormal cellular migration of astrocytes that ensheath the hyaloid artery.

Discussion

Crystallins are abundant structural proteins of the lens. However, prior studies have shown that they are also expressed outside of the lens and may have functional roles [11,36,37]. CRYBA1 is a lysosomal luminal protein in these cells and is required for normal clearance processes [31,34,38].

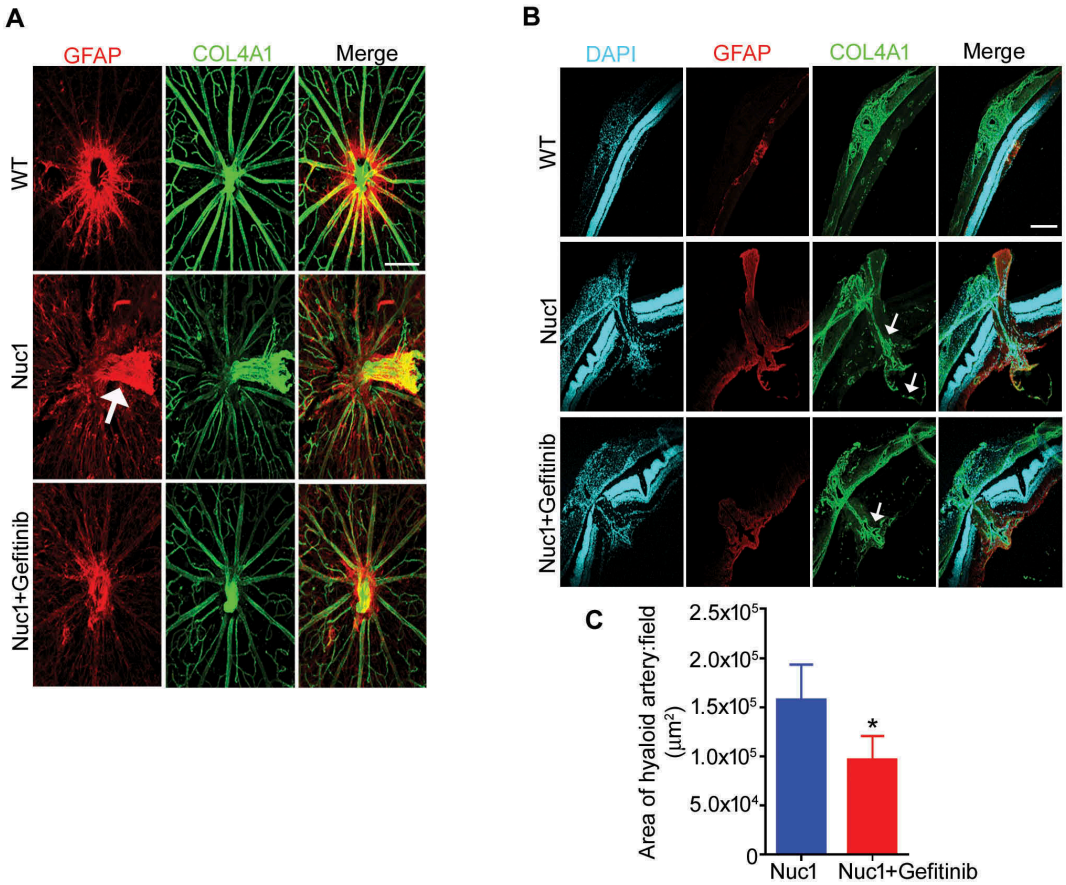

Figure 7. Gefitinib treatment promotes the regression of hyaloid artery in Nuc1 rats. (A-C) WT and Nuc1 rats were treated with gefitinib from P10 to P31. Retinal flat mounts (A) and cryosections (B,C) were immunolabelled for astrocytes and blood vessels with anti-GFAP and anti-COL4A1, respectively, and analyzed by fluorescent microscopy. DAPI staining (blue) labels the cell nuclei. (A) Astrocytes in Nuc1 migrate into the vitreous and ensheath the retained hyaloid artery (white arrow). After gefitinib treatment, the reduced GFAP-staining indicates that retention of the hyaloid artery was markedly diminished. Scale bar: 100 μm. (B,C) Representative confocal microscopy images of cryosections revealed that retention of hyaloid artery (white arrows) was decreased by gefitinib treatment. The graph indicates that the area (mm^2) of hyaloid artery was statistically significantly reduced in Nuc1 retina after gefitinib treatment relative to untreated group. Scale bar: 100 μm. Values represent mean ± S.E.M. (n = 6); * $P < 0.05$.

Importantly, we have shown that CRYBA1 is absolutely essential for normal functioning of lysosomes in astrocytes and retinal pigmented epithelium (RPE) cells [18,31,34]. Recently, a large deletion mutation responsible for removal of exons 2, 3 and 4 in *Cryba1* that causes PFV has been observed (S. Rajkumar, personal communication).

A major finding from our earlier studies is that astrocytes surround the persistent hyaloid artery both in animal models and in human PFV disease [11,23]. In the normal retina, astrocytes are confined to the nerve fiber layer [39,40]; our studies indicate that this abnormal migration of astrocytes is the key element in PFV disease. It has become clear that autophagy can regulate cell migration [41–43]. While the molecular mechanism by which the autophagy process regulates cell migration is only beginning to emerge, our studies suggest a role for EGFR, an upstream regulator of MTORC1 kinase (a known modulator of autophagy). Interestingly, an elegant study has shown that in glioma cells, cell migration is inhibited when EGFR is down-regulated and autophagy is activated [42]. It has also been shown that stimulating autophagy by inhibiting MTORC1 can slow the speed of migration in glioma cells [42,43].

While once regarded as a bag of waste disposal enzymes, lysosomes are now recognized to be an important hub for many signaling pathways, particularly MTORC1 [44,45]. It is well known that MTORC1 is a negative regulator of autophagy [46,47]. Here, we found that the autophagy process is inhibited in cultured Nuc1 astrocytes. It has been demonstrated that autophagy contributes to the regression of hyaloid vessels in early ocular development [48]. Consistently, our studies to date provide strong evidence linking impaired autophagy in astrocytes to PFV disease. Therefore, we considered inhibiting the MTORC1 pathway in these astrocytes, and thereby activating autophagy, as an innovative strategy for treating PFV. Our data suggests that rejuvenating impaired autophagy in astrocytes by inhibiting MTORC1 signaling is a viable strategy for treating PFV.

While MTORC1 has emerged as a legitimate target for therapy of various diseases [49,50], it is also true that intolerable side effects accompany the use of MTORC1 inhibitors [51]. To overcome this impediment, we looked for upstream modulators of MTORC1 to help define effective and safe treatments. We found that CRYBA1 binds to EGFR, a known upstream regulator of MTORC1. EGFR is a multifunctional glycoprotein, highly expressed in normal tissues and neoplastic lesions of most organs [52,53]. Furthermore, it plays a crucial role in cell division, migration, adhesion, differentiation and apoptosis [54,55]. EGFR is

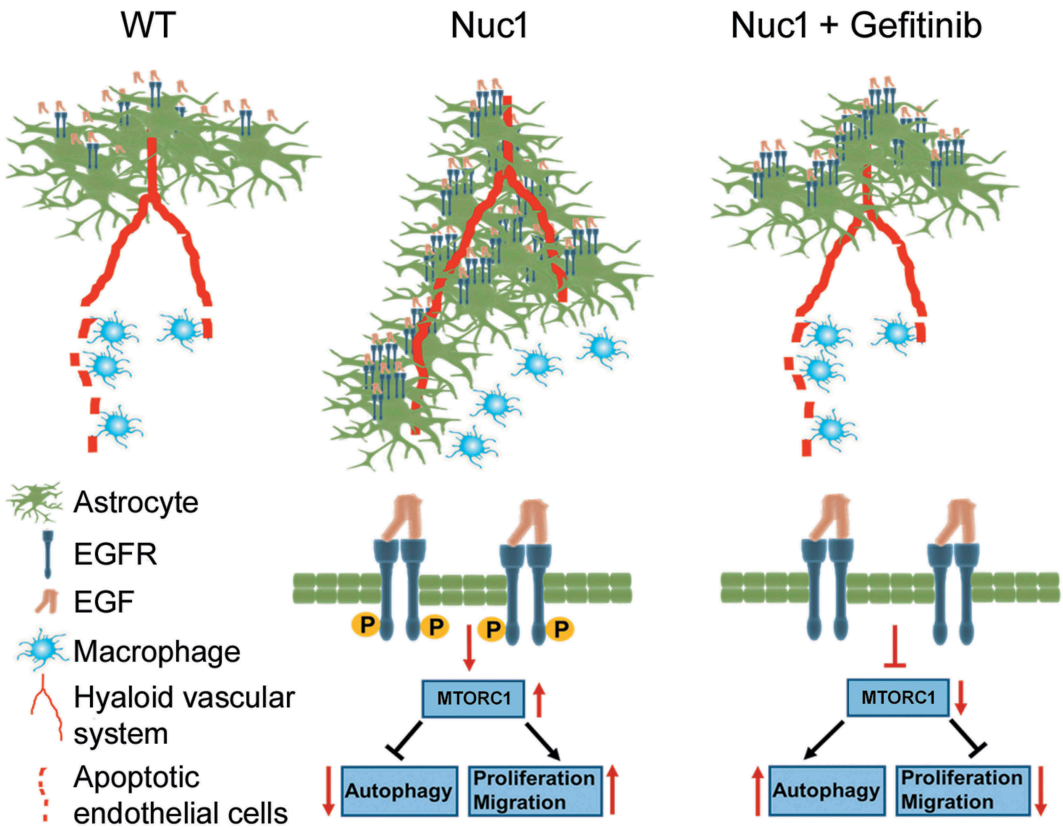

Figure 8. A graphic model demonstrating that targeting astrocytes with gefitinib triggers involution of the hyaloid vascular system in Nuc1 rats. Nuc1 is a rat model that is characterized by a complete failure of the hyaloid vasculature to regress. The rates of proliferation and migration are increased in Nuc1 astrocytes which lead to ensheathment of the hyaloid artery and inhibition of hyaloid artery regression. The level of EGFR is increased in Nuc1 astrocytes which results in over-activation of MTOR pathway and therefore downregulation of autophagy. Gefitinib reduces proliferation and migration of Nuc1 astrocytes through activation of the autophagy pathway. Gefitinib treatment leads to regression of the hyaloid vascular system in Nuc1 rats. Thus, gefitinib may be a potential therapeutic drug for treatment of PFV.

tightly regulated by complex endocytic machinery and is either recycled back to the cell surface after internalization or transported to lysosomes for degradation [56]. Further, it is known that inhibition of EGFR can block MTORC1 kinase activity [57,58]. Interestingly, gefitinib treatment not only rescued abnormal proliferation, migration, and autophagy flux in Nuc1 astrocytes, but most importantly, gefitinib significantly reduced the retention of the hyaloid artery in Nuc1 rats. Finding similar effects with the MTORC1 inhibitor rapamycin confirms the role of the EGFR-MTORC1 pathway in ameliorating PFV in this system. Since, as noted above, MTORC1 inhibitors such as rapamycin are unsuitable for clinical use, we believe that gefitinib has strong potential for the treatment of PFV disease without the side effects from directly modulating MTORC1.

We recognize that PFV is a complex and heterogeneous disease [6] and that no single therapy is likely to be effective for all patients. Gefitinib is just one potential strategy for treatment of the disease. Current treatment depends upon the severity of PFV. With mild disease, children can often be watched. With more severe disease, lensectomy and vitrectomy are needed to treat a swollen lens that can induce secondary glaucoma or traction by the accompanying fibrosis that results in vitreous hemorrhage or retinal detachment. In reality, the treatment options for children with PFV are limited and most have a poor visual outcome [6,13]. A recent study showed that genetic deletion of neuronal KDR/VEGFR2 results in PFV, possibly due to overproduction of VEGFA (vascular endothelial growth factor A) in the vitreous [59]. We have previously postulated that the severity of lens damage in PFV is a major determinant of disease severity [18]. Although astrocytes produce VEGFA during the critical time of hyaloid regression [60,61], the lens is likely to be the major source of intravitreal VEGFA in Nuc1 rats [18]. Actually, intraocular lens implantation has been beneficial in preventing progressive pathological changes in some children with PFV [62,63]. An alternative strategy for treating some severe cases may be to perform intraocular lens implantation early in life. Gefitinib is a potential strategy for treatment of PFV. With mild disease composed of a persistent vascular stalk and minimal fibrosis, gefitinib could hasten regression of the vascular stalk. With more severe disease with a fibrotic stalk, gefitinib may be given prior to vitrectomy, as with anti-VEGFA injections being given prior to vitrectomy for diabetic traction detachment to make the surgery technically simpler with reduced intraoperative and postoperative hemorrhaging [64–67]. Ultimately, with prenatal detection, gefitinib could be delivered to the baby's eye before the disabling fibrotic changes manifest. Even if a minority of patients benefit from gefitinib treatment, it would be an important therapeutic advance for a disease without effective treatment.

Materials and methods

Animals

All animal studies were conducted in accordance with the Guide for the Care and Use of Animals (National Academy Press) and were approved by the University of Pittsburgh Animal Care and Use Committee.

Astrocyte culture

Optic nerve astrocytes from 2-d-old wild type (WT) and Nuc1 rats were cultured as described previously [17].

Wound healing assay

A classical wound-healing assay was used to compare the migratory ability of WT and Nuc1 astrocytes as described previously [68]. The cell cycle blocker hydroxyurea (5 mM; Sigma–Aldrich, H8627) was added for the duration of the experiment so that the wound closure contributions of cell proliferation could be discriminated from those of cell migration. Percentage of wound healing was measured as follows: (1 – [empty area X h/empty area 0 h]) × 100. The wound healing area was analyzed with ImageJ software (NIH) and the corresponding data, relative to 0 h, expressed in the graph.

EGFR degradation assay

The EGFR degradation assay was performed as previously described [69].

Plasmids and transfection

Astrocytes were transfected with vector control pcDNA (Thermo Fisher, K80001) or pcDNA-*Cryba1* developed in our lab as described previously [18].

Proliferation assay

WT and Nuc1 astrocytes (density of 35,000 cells/cm^2) cultured from animals in our own colony were seeded on 60 mm tissue culture dishes. After 72 h, the total number of live cells (negative for trypan blue) was counted by hemocytometer and divided by the initial number of cells. In order to rescue the hyper-proliferative phenotype in the Nuc1 astrocytes following overexpression of CRYBA1, cells were seeded on 60 mm tissue culture dishes at a density of 50,000 cells/cm^2. After 24 h, cells reached 60% confluency and were transfected with pcDNA-*Cryba1* or vector control as described previously [18,70]. Fresh 1 ml medium was added to the cells 8 h after adding the transfection mixture, without removing the transfection mixture for an additional 12 h. The medium was then completely replaced with fresh medium and cells were allowed to recover for 48 h. Finally, the number of live cells was measured and divided by the initial cell number.

Cell death assay

LIVE/DEAD™ Fixable Blue Dead Cell Stain Kit (Invitrogen, L34961), a dead cell staining kit, was used to determine the level of cell death by flow cytometry, following instructions from the manufacturer.

Autophagy flux

Autophagy flux was measured by treating the WT and Nuc1 astrocytes with chloroquine (50 μM; Millipore Sigma, C6628), which inhibits acidification inside the lysosome. The ratio of LC3-II/MAP1LC3B levels in the presence and absence of chloroquine, was determined by immunoblotting as described previously [71].

Analysis of autophagosome and autolysosome formation

WT and Nuc1 cells transfected by baculovirus expressing LC3B/MAP1LC3B used to the acid-sensitive green fluorescent protein (GFP) and acid-insensitive red fluorescent protein (RFP) (Life Technologies, P36239; Premo Autophagy Tandem Sensor RFP-GFP-LC3 kit). Autophagy was induced by serum deprivation for 3 h and then, certain WT cultures were treated with 50 nM bafilomycin A_1 (Sigma, B1793) for 2 h. To analyze the expression level of SQSTM1/p62 in WT and Nuc1 astrocytes, we used the commercially available Premo Autophagy Tandem Sensor p62 Kit (Life Technologies, P36240) according to the manufacturer's protocol.

Immuno-gold/silver labeling of lysosomes in cultured rat astrocytes

WT and Nuc1 rat astrocytes were plated in separate four well chamber slides (Lab-Tek, NUNC, 177437) coated with poly-d-lysine (Sigma, P6407) until 75%-80% confluency. The cells were embedded, fixed and then blocked in these chambers as described previously [38]. Cells were washed in incubation buffer (IB) containing 10 mM phosphate buffer (PB), 150 mM NaCl, and 0.2% Aurion BSA-cTM (15 mM NaN3, pH 7.4; Electron Microscopy Sciences, 900.022), incubated overnight at 4°C in rabbit anti-EGFR antibody (Sigma, HPA018530) diluted 1:250 in IB, followed by several washes with IB. Gold labeling was accomplished with Aurion goat anti-rabbit ultra-gold (EMS), diluted 1:100 in IB and subsequently washed with it, post-fixed for 15 min (4°C) in 2% glutaraldehyde in PB, washed in PB and silver enhanced with R-gent SE-EM and conditioner (Electron Microscopy Services, 25521) according to the manufacturer's protocol. The cells were then prepared for electron microscopy using previously published method and visualized on Hitachi H7600 transmission electron microscope [38].

Western blotting and antibodies

Western blotting and quantification were performed as previously described [31,34]. The signal intensity of the detected protein was normalized to that of the housekeeping protein and analyzed using ImageJ analysis software. All targeted

proteins and internal loading controls were detected and verified within the same linear range. The primary antibodies used for western blotting in this study were LC3, GAPDH (glyceraldeyde-3-phosphate dehydrogenase), phospho-RPS6KB1 (phospho ribosomal protein S6 kinase, polypeptide 1), RPS6KB1 (ribosomal protein S6 kinase, polypeptide 1), phospho-RPS6, RPS6, EGFR, phospho-EGFR, TUBB (tubulin beta class 1), phospho-MTOR, CCND3 (cyclin D3), CDK6 (cyclin-dependent kinase 6) (Cell Signaling Technology, 2775, 5174, 9204 [phospho-RPS6KB1 Thr421/Ser424], 9234 [phospho-RPS6KB1 Thr389], 2708, 2211, 2217, 2646, 2234, 2128, 5536, 2936, and 3136), SQSTM1 (Abcam, ab91526; Novus Biologicals, NBP1-42821), ACTB (actin, beta; Sigma Aldrich, A2066), PCNA (proliferating cell nuclear antigen; NB500-106, Novus Biologicals), PARP1 (poly [ADP-ribose] polymerase family, member 1; Cell Signaling Technology, 9542), cleaved CASP3 (Cell Signaling Technology, 9664) and VCL (vinculin; Abcam, ab129002). Secondary antibodies were peroxidase labeled goat anti-rabbit and anti-mouse (KPL, 074–1506 and 074–1806).

Co-immunoprecipitation (Co-IP)

Co-IP was performed using the Pierce™ Co-Immunoprecipitation Kit (Thermo Fisher, 26149) to evaluate association between EGFR with CRYBA1 using previously published methods [34,72].

Drug delivery

For *in vitro* studies, astrocytes were treated with different concentrations (please see figure legends) of Gefitinib (Selleckchem, ZD1839) and AZD8055 (Selleckchem, S1555) in DMSO (vehicle), while control samples were treated with DMSO for 12 h. Western blotting, immunostaining, or the proliferation assays were then used for analysis of treated cells and compared to controls. Gefitinib (80 mg/kg), rapamycin (8 mg/kg) (Abcam, ab146591) and DMSO (vehicle) were injected intraperitoneally into 10-d-old WT and Nuc1 rats, three times a week for three weeks. Then, one retina from each rat was fixed for immunohistochemistry analysis, and the other retina lysed for extraction of proteins and immunoblotting analysis.

Tissue preparation

Eyes were enucleated and one eye was prepared for cryosection in OCT (Sakura Finetek, LB-4583-EA) and fellow retina was prepared for flat mount immunostaining as described [73].

Immunostaining and imaging

Cross sections or flat mount retinas were immunostained by using antibodies against GFAP (glial fibrillary acidic protein; Novus Biologicals, NBP1-05197) and COL4A1 (collagen, type IV, alpha 1; Millipore Sigma, AB756P), SQSTM1 (Abcam, ab91526) and MKI67 (antigen identified by monoclonal antibody Ki 67; Invitrogen, MA5-14520) as described previously [73]. Stereological analysis of the hyaloid artery retention was performed by analyzing the one-in-two series of 8 µm cryosections from the whole hyaloid artery. Areas of hyaloid artery retention were obtained by tracing the outline of this structure, identified by the presence of cell nuclei stained by 4′6-diamino-2-phenylindole (DAPI) and COL4A1 (a marker of blood vessels) on confocal microscopy images. The area of the hyaloid artery in each cross section was measured using ImageJ software. Six animals per group were analyzed.

Statistical analysis

Statistical analysis was performed using GraphPad 6.0 software. The *P*-values were determined by 2-tailed Student's *t*-test in a triplicate experiment representative of at least 3 independent experiments. Multiple comparisons were made using one-way ANOVA test. The level of significance was set at * $P < 0.05$; ** $P < 0.01$; *** $P < 0.001$. Results are presented as mean ± SEM. Each biological replicate has at least 3 technical replicates.

Acknowledgments

We thank Dr. Morton F. Goldberg, Wilmer Eye Institute, The Johns Hopkins University School of Medicine for critical reading and discussions regarding this manuscript. We thank Dr. S. Rajkumar, Head of Genetics, Aditya Jyot Foundation, Mumbai, India for sharing PFV patient data with a large deletion in the *Cryba1* gene. This work was supported by Knights Templar Eye Foundation (MY), NIH EY019037 (DS), University of Pittsburgh start-up funds (DS), Jennifer Salvitti Davis, M.D. Chair in Ophthalmology (DS), and an unrestricted grant from Research to Prevent Blindness to the Department of Ophthalmology, University of Pittsburgh.

Disclosure statement

No potential conflict of interest was reported by the authors.

Funding

This work was supported by the Knights Templar Eye Foundation [To Meysam Yazdankhah];National Eye Institute [NIH EY019037 to Debasish Sinha]; Jennifer Salvitti Davis Chair in Ophthalmology, UPitt [To Debasish Sinha]; Research to Prevent Blindness [Grant to UPitt Ophthalmology];University of Pittsburgh [Start-up funds to Debasish Sinha].

ORCID

Rhonda Grebe http://orcid.org/0000-0003-1841-9777

References

[1] Lang RA. Apoptosis in mammalian eye development: lens morphogenesis, vascular regression and immune privilege. Cell Death Differ. 1997;4(1):12–20.
[2] Liu C, Nathans J. An essential role for frizzled 5 in mammalian ocular development. Development. 2008;135(21):3567–3576.
[3] Selvam S, Kumar T, Fruttiger M. Retinal vasculature development in health and disease. Prog Retin Eye Res. 2018;63:1–19.
[4] Saint-Geniez M, D'Amore PA. Development and pathology of the hyaloid, choroidal and retinal vasculature. Int J Dev Biol. 2004;48:1045–1058.

[5] Zhu M, Provis JM, Penfold PL. The human hyaloid system: cellular phenotypes and inter-relationships. Exp Eye Res. 1999;68:553–563.
[6] Goldberg MF. Persistent fetal vasculature (PFV): an integrated interpretation of signs and symptoms associated with persistent hyperplastic primary vitreous (PHPV). LIV Edward Jackson Memorial Lecture. Am J Ophthalmol. 1997;124(5):587–626.
[7] Son AI, Sheleg M, Cooper MA, et al. Formation of persistent hyperplastic primary vitreous in ephrin-A5-/- mice. Invest Ophthalmol Vis Sci. 2014;55(3):1594–1606.
[8] Hegde S, Srivastava O. Different gene knockout/transgenic mouse models manifesting persistent fetal vasculature: Are integrins to blame for this pathological condition? Life Sci. 2017;171:30–38.
[9] Zhou M, Wang H, Ren H, et al. Large is required for normal astrocyte migration and retinal vasculature development. Cell Biosci. 2017;7:18.
[10] Zhang C, Gehlbach P, Gongora C, et al. A potential role for beta- and gamma-crystallins in the vascular remodeling of the eye. Dev Dyn. 2005;234(1):36–47.
[11] Zigler JS Jr, Sinha D. βA3/A1-crystallin: more than a lens protein. Prog Retin Eye Res. 2015;44:62–85.
[12] Sinha D, Klise A, Sergeev Y, et al. βA3/A1-crystallin in astroglial cells regulates retinal vascular remodeling during development. Mol Cell Neurosci. 2008;37(1):85–95.
[13] Zigler JS Jr, Valapala M, Shang P, et al. βA3/A1-crystallin and persistent fetal vasculature (PFV) disease of the eye. Biochim Biophys Acta. 2016;1860(1 Pt B):287–298.
[14] Graw J. Genetics of crystallins: cataract and beyond. Exp Eye Res. 2009;88(2):173–189.
[15] Ma Z, Yao W, Chan CC, et al. βA3/A1-crystallin splicing mutation causes cataracts by activating the unfolded protein response and inducing apoptosis in differentiating lens fiber cells. Biochim Biophys Acta. 2016;1862(6):1214–1227.
[16] Ma B, Sen T, Asnaghi L, et al. βA3/A1-crystallin controls anoikis-mediated cell death in astrocytes by modulating PI3K/AKT/mTOR and ERK survival pathways through the PKD/Bit1-signaling axis. Cell Death Dis. 2011;2:e217.
[17] Valapala M, Edwards M, Hose S, et al. βA3/A1-crystallin is a critical mediator of STAT3 signaling in optic nerve astrocytes. Sci Rep. 2015;5:8755.
[18] Valapala M, Hose S, Gongora C, et al. Impaired endolysosomal function disrupts Notch signaling in optic nerve astrocytes. Nat Commun. 2013;4:629.
[19] Zhang C, Ashaghi L, Gongora C, et al. A developmental defect in astrocytes inhibits programmed regression of the hyaloid vasculature in the mammalian eye. Eur J Cell Biol. 2011;90:440–448.
[20] Hurskainen M, Eklund L, Hägg PO, et al. Abnormal maturation of the retinal vasculature in type XVIII collagen/endostatin deficient mice and changes in retinal glial cells due to lack of collagen types XV and XVIII. Faseb J. 2005;19:1564–1566.
[21] Reneker LW, Overbeek PA. Lens-specific expression of PDGF-A in transgenic mice results in retinal astrocytic hamartomas. Invest Ophthalmol Vis Sci. 1996;37(12):2455–2466.
[22] Edwards MM, McLeod DS, Grebe R, et al. Lama1 mutations lead to vitreoretinal blood vessel formation, persistence of the fetal vasculature, and epiretinal membrane formation in mice. BMC Dev Biol. 2011;11(1):60.
[23] Sinha D, Valapala M, Bhutto I, et al. βA3/A1-crystallin is required for proper astrocyte template formation and vascular remodeling in the retina. Transgenic Res. 2012;21(5):1033–1042.
[24] Sibilia MI, Kroismayr R, Lichtenberger BM, et al. The epidermal growth factor receptor: from development to tumorigenesis. Differentiation. 2007;75(9):770–787.
[25] Lindsey S, Langhans SA. Epidermal growth factor signaling in transformed cells. Int Rev Cell Mol Biol. 2015;314:1–41.
[26] Jutten B, Rouschop KM. EGFR signaling and autophagy dependence for growth, survival, and therapy resistance. Cell Cycle. 2014;13(1):42–51.
[27] Horn D, Hess J, Freier K, et al. Targeting EGFR-PI3K-AKT-mTOR signaling enhances radiosensitivity in head and neck squamous cell carcinoma. Expert Opin Ther Targets. 2015;19(6):795–805.
[28] Mauvezin C, Neufeld TP. Bafilomycin A1 disrupts autophagic flux by inhibiting both V-ATPase-dependent acidification and Ca-P60A/SERCA-dependent autophagosome-lysosome fusion. Autophagy. 2015;11(8):1437–1438.
[29] Mizushima N, Levine B, Cuervo AM, et al. Autophagy fights disease through cellular self-digestion. Nature. 2008;451(7182):1069–1075.
[30] Rusten TE, Stenmark H. P62, an autophagy hero or culprit? Nat Cell Biol. 2010;12(3):207–209.
[31] Valapala M, Wilson C, Hose S, et al. Lysosomal-mediated waste clearance in retinal pigment epithelial cells is regulated by CRYBA1/βA3/A1-crystallin via V-ATPase-MTORC1 signaling. Autophagy. 2014;10(3):480–496.
[32] Willems L, Chapuis N, Puissant A, et al. The dual mTORC1 and mTORC2 inhibitor AZD8055 has anti-tumor activity in acute myeloid leukemia. Leukemia. 2012;26(6):1195–1202.
[33] Chresta CM, Davies BR, Hickson I, et al. AZD8055 is a potent, selective, and orally bioavailable ATP-competitive mammalian target of rapamycin kinase inhibitor with in vitro and in vivo antitumor activity. Cancer Res. 2010;70(1):288–298.
[34] Shang P, Valapala M, Grebe R, et al. The amino acid transporter SLC36A4 regulates the amino acid pool in retinal pigmented epithelial cells and mediates the mechanistic target of rapamycin, complex 1 signaling. Aging Cell. 2017;16(2):349–359.
[35] Herbst RS, Fukuoka M, Baselga J. Gefitinib–a novel targeted approach to treating cancer. Nat Rev Cancer. 2004;4(12):956–965.
[36] Piatigorsky J. Multifunctional lens crystallins and corneal enzymes. More than meets the eye. Ann N Y Acad Sci. 1998;842:7–15.
[37] Slingsby C, Wistow GJ. Functions of crystallins in and out of lens: roles in elongated and post-mitotic cells. Prog Biophys Mol Biol. 2014;115(1):52–67.
[38] Zigler JS Jr, Zhang C, Grebe R, et al. Mutation in the βA3/A1-crystallin gene impairs phagosome degradation in the retinal pigmented epithelium of the rat. J Cell Sci. 2011;124(Pt 4):523–531.
[39] Büssow H. The astrocytes in the retina and optic nerve head of mammals: a special glia for the ganglion cell axons. Cell Tissue Res. 1980;206(3):367–378.
[40] O'Sullivan ML, Puñal VM, Kerstein PC, et al. Astrocytes follow ganglion cell axons to establish an angiogenic template during retinal development. Glia. 2017;10:1697–1716.
[41] Kenific CM, Wittmann T, Debnath J. Autophagy in adhesion and migration. J Cell Sci. 2016;129(20):3685–3693.
[42] Palumbo S, Tini P, Toscano M, et al. Combined EGFR and autophagy modulation impairs cell migration and enhances radiosensitivity in human glioblastoma cells. Cell Physiol. 2014;229(11):1863–1873.
[43] Catalano M, D'Alessandro G, Lepore F, et al. Autophagy induction impairs migration and invasion by reversing EMT in glioblastoma cells. Mol Oncol. 2015;9(8):1612–1625.
[44] Lamming DW, Bar-Peled L. Lysosome: the metabolic signaling hub. Traffic. 2019;10(1):27–38.
[45] Saftig P, Haas A. Turn up the lysosome. Nat Cell Biol. 2016;18(10):1025–1027.
[46] Kroemer G, Mariño G, Levine B. Autophagy and the integrated stress response. Mol Cell. 2010;40(2):280–293.
[47] Paquette M, El-Houjeiri L, Pause A. mTOR pathways in cancer and autophagy. Cancers (Basel). 2018;10(1):18.
[48] Kim JH, Kim JH, Yu YS. Autophagy-induced regression of hyaloid vessels in early ocular development. Autophagy. 2010;6(7):922–928.
[49] Saxton RA, Sabatini DM. mTOR signaling in growth, metabolism, and disease. Cell. 2017;168(6):960–976.
[50] Sengupta S, Peterson TR, Sabatini DM. Regulation of the mTOR complex 1 pathway by nutrients, growth factors, and stress. Mol Cell. 2010;40(2):310–322.
[51] Kaplan B, Qazi Y, Wellen JR. Strategies for the management of adverse events associated with mTOR inhibitors. Transplant Rev. 2014;28(3):126–133.

[52] Furnari FB, Cloughesy TF, Cavenee WK, et al. Heterogeneity of epidermal growth factor receptor signaling networks in glioblastoma. Nat Rev Cancer. 2015;15(5):302–310.
[53] Recondo G, Facchinetti F, Olaussen KA, et al. Making the first move in EGFR-driven or ALK-driven NSCLC: first-generation or next-generation TKI? Nat Rev Clin Oncol. 2018;15(11):694–708.
[54] Liu X, Wang P, Zhang C, et al. Epidermal growth factor receptor (EGFR): A rising star in the era of precision medicine of lung cancer. Oncotarget. 2017;8(30):50209–50220.
[55] Olsen JV, Blagoev B, Gnad F, et al. Global, in vivo, and site-specific phosphorylation dynamics in signaling networks. Cell. 2006;127(3):635–648.
[56] Huber LA, Teis D. Lysosomal signaling in control of degradation pathways. Curr Opin Cell Biol. 2016;39:8–14.
[57] Han W, Pan H, Chen Y, et al. EGFR tyrosine kinase inhibitors activate autophagy as a cytoprotective response in human lung cancer cells. PLoS One. 2011;6(6):e18691.
[58] Karachaliou N, Codony-Servat J, Teixidó C, et al. BIM and mTOR expression levels predict outcome to erlotinib in EGFR-mutant non-small-cell lung cancer. Sci Rep. 2015;5:17499.
[59] Yoshikawa Y, Yamada T, Tai-Nagara I, et al. Developmental regression of hyaloid vasculature is triggered by neurons. J Exp Med. 2016;213(7):1175–1183.
[60] Scott A, Powner MB, Gandhi P, et al. Astrocyte-derived vascular endothelial growth factor stabilizes vessels in the developing retinal vasculature. PLoS One. 2010;5(7):e11863.
[61] Gerhardt H, Golding M, Fruttiger M, et al. VEGF guides angiogenic sprouting utilizing endothelial tip cell filopodia. J Cell Biol. 2003;161:1163–1177.
[62] Matsuo T. Intraocular lens implantation in unilateral congenital cataract with minimal levels of persistent fetal vasculature in the first 18 months of life. Springerplus. 2014;3:361.
[63] Sisk RA, Berrocal AM, Feuer WJ, et al. Visual and anatomic outcomes with or without surgery in persistent fetal vasculature. Ophthalmology. 2010;117(11):2178–2183.
[64] Ahn J, Woo SJ, Chung H, et al. The effect of adjunctive intravitreal bevacizumab for preventing postvitrectomy hemorrhage in proliferative diabetic retinopathy. Ophthalmology. 2011;118(11):2218–2226.
[65] El-Sabagh HA, Abdelghaffar W, Labib AM, et al. Preoperative intravitreal bevacizumab use as an adjuvant to diabetic vitrectomy: histopathologic findings and clinical implications. Ophthalmology. 2011;118(4):636–641.
[66] Farahvash MS, Majidi AR, Roohipoor R, et al. Preoperative injection of intravitreal bevacizumab in dense diabetic vitreous hemorrhage. Retina. 2011;31(7):1254–1260.
[67] Hernández-Da Mota SE, Nuñez-Solorio SM. Experience with intravitreal bevacizumab as a preoperative adjunct in 23-G vitrectomy for advanced proliferative diabetic retinopathy. Eur J Ophthalmol. 2010;20(6):1047–1052.
[68] Liang CC, Park AY, Guan JL. In vitro scratch assay: a convenient and inexpensive method for analysis of cell migration in vitro. Nat Protoc. 2007;2(2):329–333.
[69] Pinilla-Macua I, Sorkin A. Methods to study endocytic trafficking of the EGF receptor. Methods Cell Biol. 2015;130:347–367.
[70] Gadea A, Schinelli S, Gallo V. Endothelin-1 regulates astrocyte proliferation and reactive gliosis via a JNK/c-Jun signaling pathway. J Neurosci. 2008;28(10):2394–2408.
[71] Yazdankhah M, Farioli-Vecchioli S, Tonchev AB, et al. The autophagy regulators Ambra1 and Beclin 1 are required for adult neurogenesis in the brain subventricular zone. Cell Death Dis. 2014;5(9):e1403.
[72] Ghosh S, Shang P, Yazdankhah M, et al. Activating the AKT2-nuclear factor-κB-lipocalin-2 axis elicits an inflammatory response in age-related macular degeneration. J Pathol. 2017;241(5):583–588.
[73] McLeod DS, Hasegawa T, Prow T, et al. The initial fetal human retinal vasculature develops by vasculogenesis. Dev Dyn. 2006;235(12):3336–3347.